

Oxygen dependence of the magnetic anomalies in $\text{Pr}_{1.5}\text{Ce}_{0.5}\text{Sr}_2\text{NbCu}_2\text{O}_{10}$

I. Felner

Racah Institute of Physics, The Hebrew University, Jerusalem, 91904 Israel
and Laboratoire CRISMAT, Institut des Sciences de la Matière et du Rayonnement, Université de Caen,
boulevard du Marechal Juin, 14050 Caen Cedex, France

U. Yaron and U. Asaf

Racah Institute of Physics, The Hebrew University, Jerusalem, 91904 Israel

T. Kröner and V. Breit

Kernforschungszentrum, Karlsruhe Institut für Technische Physik, P.O. Box 3640, 76021 Karlsruhe, Germany

(Received 9 August 1993)

We investigated $\text{Pr}_{1.5}\text{Ce}_{0.5}\text{Sr}_2\text{NbCu}_2\text{O}_{10}$ and the superconducting $\text{Eu}_{1.5}\text{Ce}_{0.5}\text{Sr}_2\text{NbCu}_2\text{O}_{10}$ materials by several complementary experimental techniques. Oxygen-rich $\text{Pr}_{1.5}\text{Ce}_{0.5}\text{Sr}_2\text{NbCu}_2\text{O}_{10}$ is not superconducting and the magnetic-susceptibility data reveal two magnetic anomalies at 11 and 54 K. Both anomalies always appear together and are sensitive to oxygen concentration, whereas for oxygen-poor material both anomalies are absent. The presence of 0.5% Fe dramatically affects only the transition at 54 K and shifts it to 94 K, and Mössbauer studies indicate that this transition is related to antiferromagnetic ordering of the Cu sublattice. The peak in the susceptibility at 11 K is probably due to spin reorientation of Cu moments. While the anomalies are clearly identified by magnetic measurements, no specific-heat anomaly was observed at either temperature. A strong two-dimensional quantum spin fluctuation is assumed as the cause of the unusual behavior at T_N of Cu. A high linear term of 265 mJ/mol Pr K^2 is obtained in the specific heat of the oxygen-rich $\text{Pr}_{1.5}\text{Ce}_{0.5}\text{Sr}_2\text{NbCu}_2\text{O}_{10}$ material.

INTRODUCTION

Among the compounds prepared by substitution of rare earth (R) for Y in $\text{YBa}_2\text{Cu}_3\text{O}_7$ (YBCO), with retention of the superconducting orthorhombic phase, the Pr-substituted material is an exception. Most of the $\text{RBa}_2\text{Cu}_3\text{O}_7$ (RBCO) compounds have an orthorhombic perovskitelike structure and exhibit superconductivity with $T_c \sim 90$ K. On the other hand, $\text{PrBa}_2\text{Cu}_3\text{O}_7$ (PrBCO_7) is an antiferromagnetic (AFM) insulator which possesses an unusually high $T_N(\text{Pr}) = 17$ K.¹⁻³ This T_N is about two orders of magnitude higher than expected if one scales the T_N for $\text{GdBa}_2\text{Cu}_3\text{O}_7$ ($T_N = 2.2$ K) assuming either purely dipolar interactions or simple Ruderman-Kittel-Kasuya-Yosida exchange. This T_N is very sensitive to oxygen content and reduces to roughly 10 K in the tetragonal oxygen-poor PrBCO_6 material.⁴ In addition to the Pr sublattice, using the Mössbauer technique on Fe-doped samples, we have shown² that the $\text{Cu}(2)\text{-O}_2$ layers are AFM ordered at 325 and 350 K for PrBCO_7 and PrBCO_6 respectively; thus $T_N(\text{Cu})$ varies little with oxygen concentration. A variety of unusual physical phenomena exhibited by PrBCO_7 have generated much research activity and were discussed at length in Ref. 3.

Complete replacement⁵ of the $\text{Cu}(1)\text{-O}$ chains in RBCO with NbO_6 octahedra, offered a unique opportunity to investigate the importance of the chain sites which provide carriers to the $\text{Cu}(2)\text{O}_2$ planes. In $\text{RBa}_2\text{NbCu}_2\text{O}_8$ (RBNCO) superconductivity was not found for any R investigated, due to lack of the carriers needed.^{6,7} More-

over, recent magnetic studies have shown that both Pr and Cu sublattices in $\text{PrBa}_2\text{NbCu}_2\text{O}_8$ are AFM ordered at 11.6 and 360 K respectively,^{8,9} whereas $T_N(\text{Nd})$ for $\text{NdBa}_2\text{NbCu}_2\text{O}_8$ is only 1.7 K,⁹ which is reminiscent of the situation in RBCO.

A phase resembling the RBNCO materials with the formula $\text{R}_{1.5}\text{Ce}_{0.5}\text{Sr}_2\text{NbCu}_2\text{O}_{10}$ (RCeSNCO) has been reported recently by several authors.¹⁰⁻¹³ This structure (Fig. 1) is derived from RBNCO, and the space group is $I4/mmm$ with two formula units (f.u.) in each unit cell. In contrast to RBCO, only one distinct Cu site exists with fivefold pyramidal coordination. These CuO_2 layers are separated on one side by NbO_6 octahedra which replace the Cu-O chains and on the other side by fluorite-structure $\text{R}_{1.5}\text{Ce}_{0.5}\text{O}_2$ layers (instead of the R layer in RBCO). It appears that in RCeSNCO (as in RBCO) for $R = \text{Nd, Sm, Eu, and Gd}$, the compounds are superconductors with $T_c \sim 28$ K regardless of R . On the other hand, $(\text{Pr}_{1.5}\text{Ce}_{0.5})\text{Sr}_2\text{NbCu}_2\text{O}_{10}$ (PrCeSNCO) is not superconducting, and magnetic studies at low fields reveal two anomalies in the susceptibility curve at 17 and 53 K.¹¹ In analogy to PrBCO_7 , it was proposed that the low-temperature peak is associated with AFM ordering of the Pr sublattice, whereas the unexpected peak at 53 K was not understood.¹¹

The main purpose of this paper, based on several experimental techniques, is to present a view of the two magnetic transitions in PrCeSNCO. We show that for oxygen-rich materials both peaks always appear together, and are sensitive to oxygen concentration. On the other

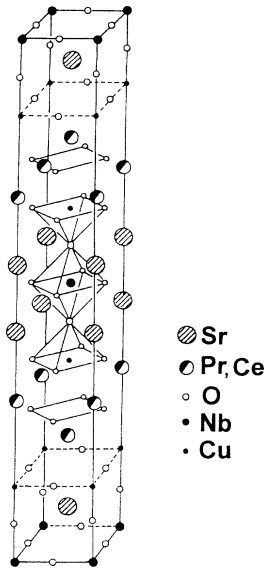


FIG. 1. Crystal structure of $\text{Pr}_{1.5}\text{Ce}_{0.5}\text{Sr}_2\text{NbCu}_2\text{O}_{10}$.

hand, neither of the two transitions is observed in oxygen-poor PrCeSNCO samples. Unexpectedly, the presence of Fe drastically affects the peak at 54 K, which is shifted to 74 or 94 K, whereas the low-temperature peak remains at 11 K. Mössbauer spectroscopy (MS) studies show that the peak at high temperatures is due to the Cu sublattice. The most striking observation is that specific-heat studies do not show any anomaly at either magnetic transition, as would be expected for AFM phase transitions. The absence of the anomaly in C_p is discussed. High γ values of 265 and 108 mJ/mol Pr K² were obtained for oxygen-rich and oxygen-poor PrCeSNCO respectively.

EXPERIMENTAL DETAILS

Ceramic samples with nominal composition ($R_{1.5}\text{Ce}_{0.5}\text{Sr}_2\text{NbCu}_2\text{O}_{10}$ and the ^{57}Fe -doped material) were prepared by the solid-state reaction technique. Prescribed amounts of Pr_6O_{11} , CeO_2 , SrCO_3 , Eu_2O_3 , Nb_2O_5 , CuO , and $^{57}\text{Fe}_2\text{O}_3$ were mixed and pressed into pellets and preheated to 1000°C for about 1 day in the presence of flowing oxygen at atmospheric pressure. The products were cooled, reground, and sintered at 1150°C for 72 h in slightly pressurized oxygen (about 1.2 atm) and then furnace cooled to ambient temperature. The PrCeSNCO sample prepared in this manner is denoted as sample (I). Two ^{57}Fe -doped samples (substituted for Cu) have been prepared using the same conditions. A part of sample (I) [the high-oxygen-pressure (HOP) sample] was reheated for 10 h at 1000°C under pure oxygen pressure at 130 atm, using a VAS high-pressure furnace. For the oxygen-deficient PrCeSNCO, referred to as sample (II), the second stage of sintering was performed at 1050°C under flowing oxygen at ambient pressure. Powder x-ray-diffraction (XRD) measurements indicate that all materials are single phase (~97%) and have the tetragonal structure shown in Fig. 1.

The oxygen weight-loss determination was performed with a Setaram microbalance TGA 24, with a heating rate of 6°/min up to 1000°C in Ar atmosphere. The dc magnetic measurements on solid ceramic pieces in the range 5–200 K were performed on a commercial (Quantum Design) superconducting quantum interference device magnetometer. The magnetization was measured by two different procedures: (a) The sample was zero-field cooled (ZFC) to 5 K, a field was applied, and the magnetization was measured as a function of temperature. (b) The sample was field cooled (FC) from above 120 to 5 K and the magnetization was measured. The MS studies were carried out using a conventional constant-acceleration spectrometer and a 50-mCi ^{57}Co :Rh source. The specific heat of compact pieces (about 100 mg) cut from the pellets was measured with a semiadiabatic heat-pulse calorimeter at $H=0$ T in the range 1.5–30 K, and a continuous adiabatic heating calorimeter in the range 20–300 K.

EXPERIMENTAL RESULTS

A. Lattice parameters and oxygen content

X-ray-diffraction studies show that the compounds have a tetragonal structure (Fig. 1) with the space group $I4/mmm$. The lattice parameters for PrCeSNCO samples are $a=3.887(1)$ and $c=28.74(1)$ Å. Within the limits of the uncertainty, all the PrCeSNCO samples studied have the same lattice constants. For EuCeSNCO the lattice parameters are $a=3.866(1)$ and $c=28.72(1)$ Å. These lattice parameters and the atomic positions determined by Rietveld analysis of the full XRD pattern are in excellent agreement with data published in Ref. 11. The iron-doped materials have approximately the same lattice parameters as their parent compounds. The Cu atoms reside in the $4e$ atomic position $(0,0,z)$ and for $z=0.144$, the shortest Cu-Cu distance is ~6.09 Å, which is shorter than the 6.55 Å observed in $\text{La}_{2-x}\text{Sr}_x\text{CuO}_4$ but much longer than the 3.52 and 3.41 Å for Cu(2)-Cu(2) distances in RBCO and PrBNCO respectively.

The weight-loss curves of PrCeSNCO measured by thermogravimetric analysis (TGA) for samples (I) and (II) are shown in Fig. 2. For sample (I) the weight decrease begins around 380°C and is completed at 660°C. The weight loss of 2.04% corresponds to an oxygen loss of 1.05(2) atoms per mole (f.u.). For the oxygen-deficient sample (II) the weight loss, which occurs in two steps, from 420 to 850°C and from 850 to 1000°C, is 0.25% and 0.5% corresponding to an oxygen loss of 0.13 and 0.27 atoms per mole respectively. Our measurements reveal that sample (I) contains about 0.6 more oxygen than sample (II), which is critical to the occurrence of its unusual magnetic behavior. It should be added that an oxygen loss of 0.13 atom was found at 600°C for superconducting NdCeSNCO (Ref. 12), which compares well with the first step observed for sample (II). After cooling the materials to room temperature, XRD measurements show decomposition of the tetragonal structure mainly to RSr_2NbO_6 ($R=\text{Pr,Ce}$) and to other unidentified phases. For the HOP sample one step from 350 to 740°C was observed in the TGA curve, which relates to a weight loss

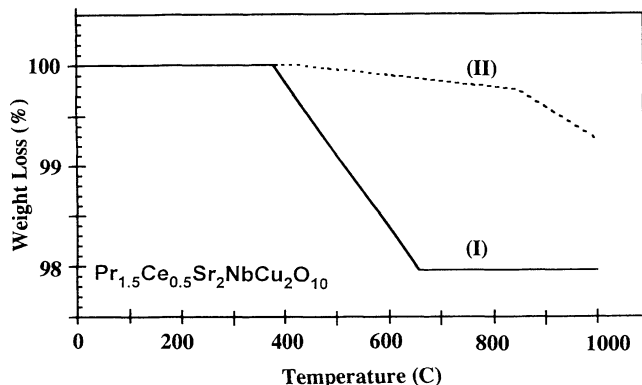


FIG. 2. Change of oxygen content of sample (I) and sample (II). The samples were heated under Ar with a rate of 6 °C/min.

of 2.51 oxygen atoms per mole. Determination of the absolute oxygen content in these materials is difficult,¹² because CeO₂ and Nb₂O₅ are not completely reducible to stoichiometric oxides on heating to high temperatures.

B. Magnetic measurements

The ZFC magnetic susceptibility [$\chi(T) \equiv M/H$] of PrCeSNCO sample (I) was measured at 40 Oe up to 200 K and Fig. 3 shows two distinct peaks at 10.7 and 54 K. No other anomalies were observed at higher temperatures. The inset of Fig. 3 provides an expanded view of $\chi(T)$ from 5 to 20 K. A similar magnetic behavior was obtained by Goodwin, Radousky, and Shelton¹¹ and the anomaly at 54 K is in perfect agreement with their data (53 K). However the peak at ~11 K (inset of Fig. 3) is somewhat lower than the 17 K reported in Ref. 11. Based on the similarity in structures of PrBCO₇, PrBNCO, and PrCeSNCO, these authors associated the low-temperature transition with an AFM ordering of the

Pr sublattice, whereas the anomaly at 53 K was not understood. Their speculation attributed it to the presence of two rare-earth ions (Pr and Ce) at the same crystallographic position. As we shall argue, the peak at 54 K is associated with AFM ordering of the Cu sublattice and the low-temperature transition may be related to Cu-Cu and Pr-Cu interactions and not to AFM ordering of the Pr sublattice. Figure 3 also shows that the position of the two peaks is sensitive to heat treatment of the material. For PrCeSNCO (I) after heat treatment at 1000 °C under 130 atm of oxygen (HOP) the low-temperature peak is shifted to ~15 K whereas T_N of the Cu sublattice is lowered to 50 K.

For the Mössbauer-spectroscopy studied, two different PrCeSNCO samples doped with 0.5 at. % ⁵⁷Fe (nominal concentration) have been prepared identically. Mössbauer studies, described in detail in the next section, show that Fe occupies mainly the Cu site. Unexpectedly, ZFC susceptibility measurements show that the peak at $T_N(\text{Cu}) = 54$ K is shifted to 94 and 74 K for samples designated samples Fe(I) and Fe(II) respectively (Fig. 4), whereas the low-temperature peak remains at about 11 K. The $\chi(T)$ curve of pure PrCeSNCO is also shown for comparison. In that respect, Fe behaves differently as compared to other high- T_c systems, in which doping with a small amount of Fe does not have a pronounced effect on $T_N(\text{Cu})$.¹⁴ Since Fe has a larger valence than Cu, it attracts oxygen to maintain neutrality, and it is also possible that this slight extra oxygen content dramatically affects $T_N(\text{Cu})$.

On the other hand, magnetic measurements performed at low and high applied fields on the oxygen-poor sample (II) show that both anomalies in $\chi(T)$ are absent. The susceptibility exhibits paramagnetic behavior down to 3 K and a typical $\chi(T)$ measured at 100 Oe is exhibited in Fig. 5. Note that the curves for samples (I) and (II) merge at $T > 90$ K, a temperature which is about 40 K

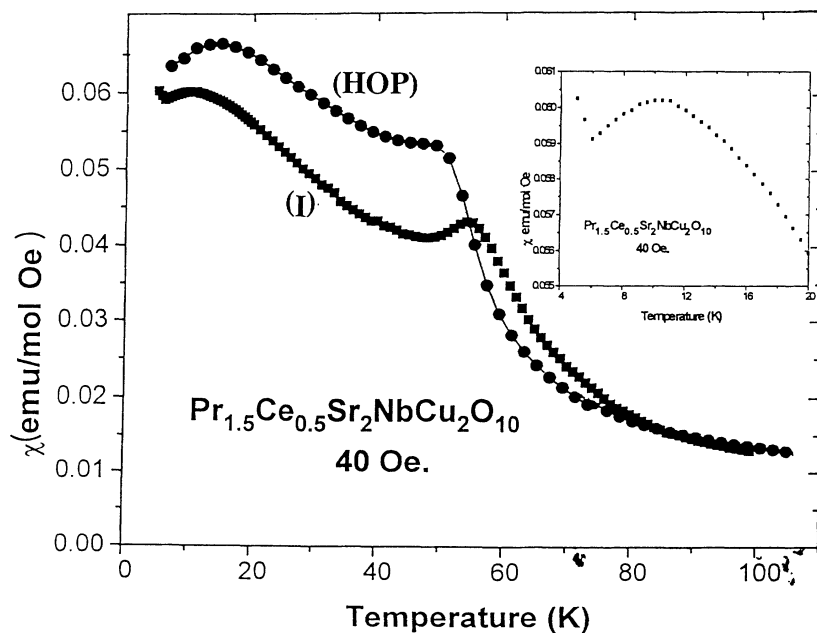


FIG. 3. Temperature dependence of the ZFC susceptibility for PrCeSNCO sample (I) and for the same sample heated at 1000 °C under 130 atm O₂ (HOP). The inset exhibits the susceptibility of PrCeSNCO sample (I) in an expanded scale.

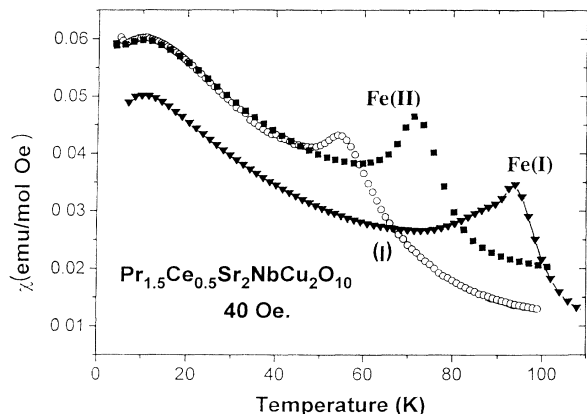


FIG. 4. Temperature dependence of the ZFC susceptibility for two samples with 0.5 at. % Fe doped in PrCeSNCO, and for PrCeSNCO.

above $T_N(\text{Cu})=54$ K. The “net” magnetic features of sample (I) can be achieved by subtraction of $\chi(T)$ of sample (II) as a background susceptibility. Figure 5 (inset) shows the $\Delta\chi$ obtained, and the smeared increase of $\Delta\chi$ with a peak at $T=18$ K and the sharp peak at 54 K are readily observed. The $\Delta\chi$ values for $T > 90$ K are small and negligible and arise from accumulation of uncertainties in the experimental data (weight, temperature, applied fields, etc.).

The effect of field strength on the position of the peaks of sample (I) is significant. Figure 6 shows typical ZFC $\chi(T)$ curves obtained at medium (500 Oe) and high (10 kOe) applied fields, together with the low-field curve (40 Oe). At 500 Oe the low-temperature transition disappears and the peak at 54 K, which is very prominent at 40 Oe, is nearly suppressed. At 10 kOe neither peak is seen; however the peak at $T_N=54$ K is clearly observed in the temperature dependence of the inverse molar susceptibility shown in the inset. Here again all the curves

merge at $T > 90$ K, which indicates that the magnetization is not linear with the applied field at lower temperatures.

Figure 7 shows the ZFC and FC susceptibility curves measured at 100 Oe for PrCeSNCO, sample (I). The irreversibility probably arises from the AFM alignment of the Cu sublattice. It is assumed that in the FC process the external field causes the spins to cant slightly out of their original direction. This canting abruptly aligns a component of the moments with the direction of the field and the FC branch is obtained. Note the absence of the peak at 11 K in the FC branch and that both FC and ZFC curves merge at 74 K. The field dependence of the magnetization at 60 K (not shown) was measured up to 5 T. At low fields the magnetization is not linear and a finite M is obtained after extrapolation of high-field data to $H=0$. This indicates the existence of an internal magnetic field (above T_N) estimated as a few hundred gauss at 60 K, which vanishes at $T > 90$ K. We shall address this point in the discussion.

Sample (I) exhibits normal paramagnetic behavior above T_N and adheres closely to the Curie-Weiss law over the major portion of the measured temperatures. The susceptibility can be well described by $\chi = \chi_0 + C/(T - \Theta)$, where χ_0 is the temperature-independent part of the susceptibility, C is the Curie constant, and Θ is the Curie-Weiss temperature. The extracted values strongly depend on the temperature range of the fitting. A fit of the Curie-Weiss law in the range of $60 < T < 100$ K measured at $H=1$ T yields $\chi_0 = 5 \times 10^{-3}$ emu/mol Oe, $\Theta = 25$ K, and an effective moment $P_{\text{eff}} = 2.53\mu_B$ for Pr. This P_{eff} value perfectly fits the value reported in Ref. 11 and the expected value ($2.54\mu_B$) for Pr^{4+} in its $J = \frac{5}{2}$ ground state. However, a fit in the range $80 < T < 200$ K yields $P_{\text{eff}} = 1.60\mu_B$ and $\Theta = 46$ K. This suppression suggests an influence of crystal field effects (CFE) on the magnetic properties at elevated temperatures and is consistent with P_{eff} values found for PrBaO_3 where Pr is assumed to be in the tetra-

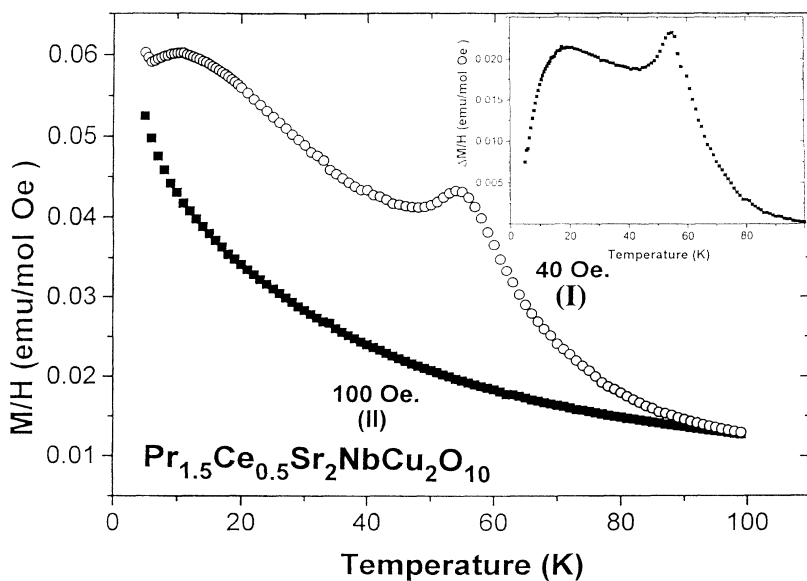


FIG. 5. Temperature dependence of the ZFC susceptibility for PrCeSNCO samples (I) and (II). The net magnetic susceptibility for sample (I) is shown in the inset.

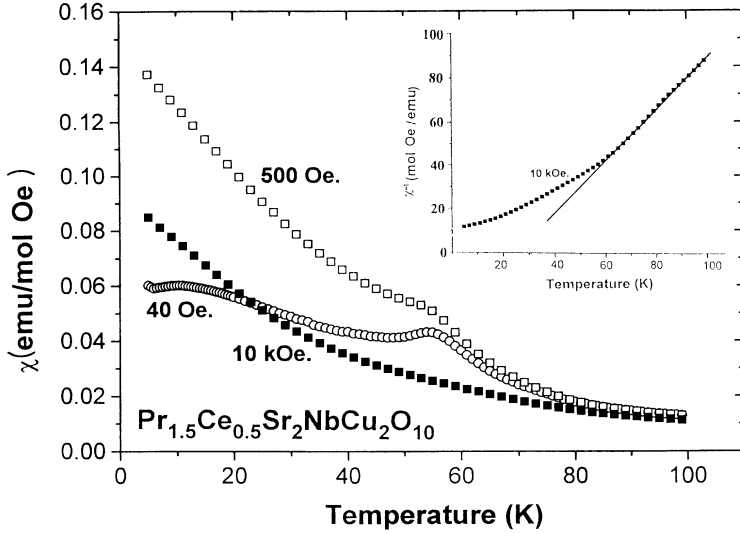


FIG. 6. Temperature dependence of the susceptibility for PrCeSNCO sample (I), measured at different fields. Note that all the curves merge at $T > 90$ K, well above $T_N = 54$ K. The inset shows the inverse molar susceptibility as a function of temperature measured at 10 kOe.

valent state.¹⁴ Note the positive value of Θ , which indicates that the exchange interactions are ferromagnetic in nature. From a similar analysis for sample (II) (Fig. 5), which is paramagnetic all the way down to 3 K, we obtain that $\chi_0 = 2.1 \times 10^{-4}$ emu/mol Oe, $\Theta = -25$ K, and $P_{\text{eff}} = 2.86\mu_B$. This P_{eff} value, although lower than the $3.5\mu_B$ expected for Pr^{3+} , is in excellent agreement with effective moments reported for PrBNCO,⁶⁻⁸ but is somewhat higher than the $2.70\mu_B$ found for PrBCO₇.¹⁵ The reduced P_{eff} in all these compounds is presumably due to the action of CFE which is assumed to have the same origin for Pr^{3+} materials. Thus, the magnetic measurements show that the extra oxygen observed in sample (I) is accompanied by an increase in the valence state of Pr.

C. The AFM sublattice of Cu: Mössbauer studies

Using Mössbauer spectroscopy on ⁵⁷Fe-doped materials, we found the interrelation between superconductivity and antiferromagnetism in a wide family of cation substitutions in the oxygen-rich YBCO system. It was shown¹⁶ that whenever cations are doped in sites outside the Cu(2)

plane, sufficiently to make superconductivity disappear [e.g., Pr in the Y site or Fe in the Cu(1) site], static long-range AFM ordering is induced in these planes. It is well accepted that in YBCO Fe atoms predominantly occupy the Cu(1) sites. A fraction of the Fe enters the Cu(2) sites and when these planes become magnetically ordered they produce an exchange field on the Fe ions located in the planes. The Fe nuclei experience a magnetic hyperfine field leading to a sextet in the observed MS spectra. Measurements² on PrBCO₇ and PrBCO₆ compounds have shown that the Cu(2) sublattice is AFM ordered at 325 and 350 K respectively; thus T_N varies little with oxygen concentration. We have also shown⁸ that the CuO₂ planes in PrBNCO are AFM ordered at 360 K. The present studies show that the RCeSNCO system behaves in a way which is similar to other high-temperature superconductors, namely, in the compositions which are not superconducting, a long-range AFM ordering is induced in the CuO₂ planes. We shall present here MS studies on ⁵⁷Fe doped in superconducting EuCeSNCO and in PrCeSNCO [sample Fe(I)], which exhibit the second peak at 94 K (Fig. 4).

1. EuCeSNCO

Magnetization studies from 5 to 40 K in an applied field of $H < 5$ Oe show an onset of superconductivity at $T_c = 18$ K for 0.5 at. % ⁵⁷Fe doped in EuCeSNCO (Fig. 8). Due to uncertainty in the applied field, the susceptibility is given in arbitrary units but an estimation yields a shielded fraction of about 20%, indicating the presence of bulk superconductivity. The Meissner fraction is smaller ($\sim 30\%$) than the ZFC signal. The value of $T_c = 18$ K for the 0.5 at. % Fe-doped sample compares well with $T_c = 22$ K obtained for undoped RCeSNCO prepared at 1 atm of oxygen.¹² It is possible that the 0.5 at. % Fe suppresses T_c . We used this sample also for our specific-heat measurement presented in the next section.

The MS spectrum of ⁵⁷Fe in superconducting EuCeSNCO at 4.2 K is shown in Fig. 9(a). We obtain one quadrupole doublet with a splitting of $eqQ/2 = 0.90(2)$ mm/sec and isomer shift of $0.35(1)$ mm/sec relative to Fe

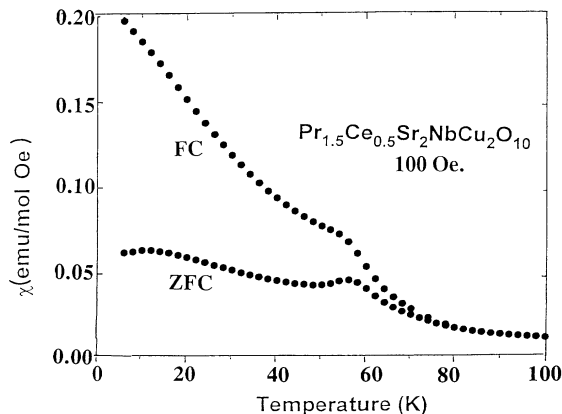


FIG. 7. ZFC and FC susceptibility curves for PrCeSNCO measured at 100 Oe.

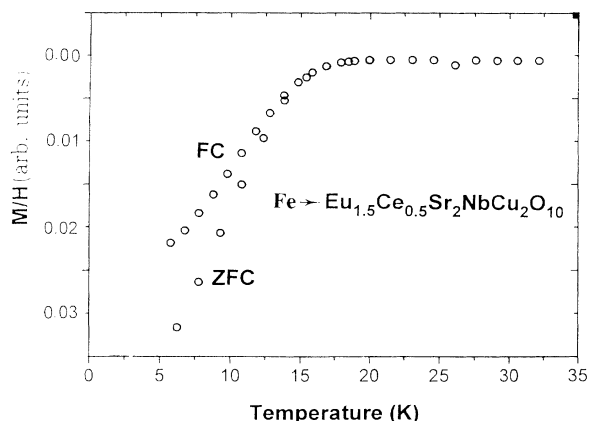


FIG. 8. ZFC and FC susceptibility in arbitrary units for the superconducting $\text{Eu}_{1.5}\text{Ce}_{0.5}\text{Sr}_2\text{NbCu}_2\text{O}_{10}$.

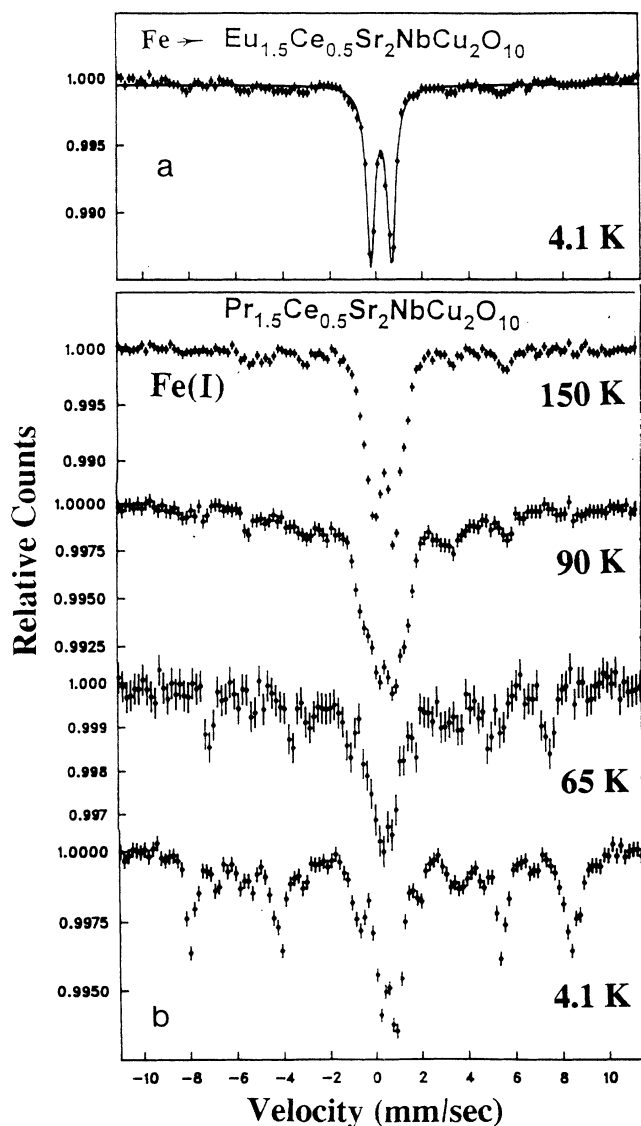


FIG. 9. Mossbauer spectra of 0.5 at.% ^{57}Fe doped in PrCeSNCO [sample Fe(I)] and of the superconducting $\text{Eu}_{1.5}\text{Ce}_{0.5}\text{Sr}_2\text{NbCu}_2\text{O}_{10}$. Note the pronounced difference between the two materials.

metal. The width is 0.44(1) mm/sec. These parameters can be assigned to Fe^{3+} in a high-spin state [the spectrum also contains minor additional peaks (less than 5%) which are attributed to an unidentified impurity phase]. We attribute this doublet to iron which replaces Cu in the pyramidal site (Fig. 1), and these hyperfine parameters compare well with data obtained in other materials such $\text{La}_2\text{CuCu}_2\text{O}_6$ with similar CuO_5 configuration.¹⁷ The relatively broad width may be related either to paramagnetic spin-relaxation phenomena existing at 4.1 K, or to a small distribution in the quadrupole interaction values. However, this is of little interest in our present discussion.

2. PrCeSNCO

The main effect to be seen in Fig. 9(b) is the MS of Fe doped in PrCeSNCO [sample Fe(I)] at various temperatures. The solubility limit of Fe seems to be small and all attempts to get better samples failed. Although we display a "dirty" material useful information concerning the nature of the Cu sublattice can be deduced and the MS will be treated qualitatively. The spectra in Fig. 9(b) consist of, at least, three subspectra. The most intense subspectrum ($\sim 60\%$) is a sextet which we attribute to iron ions, which replace Cu in the CuO_5 pyramids and order antiferromagnetically. In this site all the iron ions are equivalent in terms of oxygen environment and yield a well-defined magnetic spectrum with a magnetic hyperfine field at 4.1 K of $H_{\text{eff}} = 510(5)$ kOe. As the temperature is raised, the magnetic splitting decreases and disappears at $T > 100$ K. The values for H_{eff} at 50 and 65 K are 475(5) and 460(5) kOe respectively. At 90 K, a few degrees below $T_N(\text{Cu}) = 94$ K (Fig. 4) for sample Fe(I), the sextet starts to collapse but it is still observable. The existence of a magnetic hyperfine field at 90 K is a direct proof that peaks at 94 K [and 54 K for PrCeSNCO sample (I)] are associated with AFM ordering of the Cu sublattice. The spectrum obtained at 110 K (not shown) is very similar to the spectrum obtained at 150 K [Fig. 9(b)]. Similar behavior was observed in the sample Fe(II).

The next most intense subspectrum (about 30% of the spectral area) is not ordered magnetically, and is attributed to Fe in the sixfold octahedral Nb site, consistent with the behavior of Fe doping in the Cu(1) site of YBCO. This subspectrum (in the central part) exhibits at 4.1 K a broad quadrupole doublet corresponding to inequivalent Fe sites due to different oxygen neighbor configurations at the Nb site. Since Fe has a lower valence than Nb, it depletes oxygen to maintain neutrality. It is assumed that (in contrast to EuCeSNCO) Fe in PrCeSNCO occupies both Cu and Nb crystallographic sites, a phenomenon observed also in PrBNC0.⁸ However, the possibility that the doublet arises from an impurity phase cannot be excluded. The rest of the spectral area ($\sim 10\%$) contains several sextets which are magnetically ordered up to $T > 370$ K (one, which collapses at ~ 240 K, corresponds probably to Fe in Pr_2CuO_4) and are attributed to unidentified impurity phases.

In conclusion, the pronounced difference between the MS of superconducting EuCeSNCO and PrCeSNCO, in

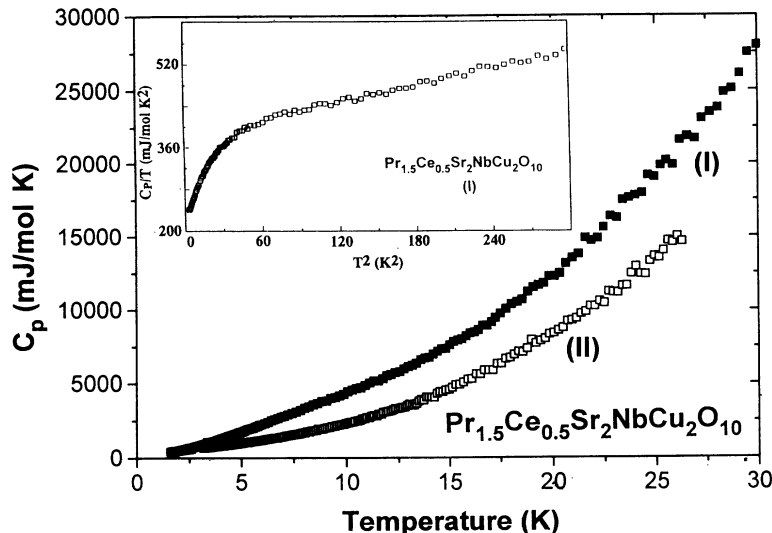


FIG. 10. Specific-heat curves at $H=0$ T for PrCeSNCO samples (I) and (II). In the inset is the C_p/T vs T^2 representation for sample (I) showing the γ value.

particular the appearance of a well-defined sextet at $T < 100$ K in PrCeSNCO, indicates clearly the existence of magnetic order in the Cu sublattice. Thus the RCeSNCO system behaves in a way which is similar to other high- T_c series, namely, in those compositions which are not superconducting, a static magnetic ordering of the Cu-O₂ planes is present.

D. Specific heat measurements

Shown in Figs. 10–12, are the C_p vs T curves for PrCeSNCO samples (I) and (II) and EuCeSNCO. In order to reveal the nature of the two peaks observed in PrCeSNCO sample (I) (Figs. 3–7) the specific heat at $H=0$ T was measured in two steps, in the ranges $1.5 < T < 35$ K and $25 < T < 300$ K. For PrCeSNCO sample (I), we find that in the vicinity of the two peaks observed in the susceptibility curves, namely, at 11 and 54 K, no specific-heat features indicative of magnetic origin can be observed. This is not the case in other Pr-based cuprates such as PrBCO₇,^{2,15} PrBNCO,⁸ and PrBaO₃,¹⁴ in which the Pr sublattices order antiferromagnetically at $T_N=10$ –17 K and a sharp anomaly in C_p is obtained at T_N . This suggests that the peak at 11 K does not originate from long-range ordering of Pr. Moreover, there is no anomaly in the C_p curve at $T_N=54$ K related to the Cu sublattice, as would be expected for an AFM order of the Cu sublattice (Fig. 11). We shall refer to these facts in the discussion.

The fitting of the C_p curve for PrCeSNCO sample (I) at low temperatures may lead to several acceptable mathematical solutions, the reliability factors of which appear to be close. The large values and the approximately linear temperature dependence of C_p (at low temperatures) suggest mainly an electronic contribution. Therefore, a fit in the range $2 < T < 25$ K with the sum of a linear term for the electronic contribution and a Debye approximation for the lattice contribution, $C_p = \gamma T + \beta T^3 + \delta T^5$, yields $\gamma = 386(3)$ mJ/mol K², $\beta = 0.582$ mJ/mol K⁴, corresponding to $\theta_D = 384(5)$ K, and $\delta < 10^{-6}$ which is negligible. The value of $\gamma = 382(3)$

mJ/mol K² was calculated by the usual procedure of extrapolating the linear variation of C_p/T versus T^2 from high temperatures to $T=0$ (Fig. 10, inset). A similar fit procedure to $C_p(T)$ of sample (II) in the range $2 < T < 25$ K yields $\gamma = 170$ mJ/mol K² and $\beta = 0.596$ mJ/mol K⁴, corresponding to $\theta_D = 381(5)$ K. Thus, the two curves differ only in their γ values. The θ_D obtained is consistent with the average value suggested for YBCO (410 ± 35 K).¹⁸

An alternative (and more elegant) way to calculate the Pr contribution to $C_p(T)$ for sample (I) (ΔC_p) is shown in the inset of Fig. 12. The linear variation of ΔC_p with T was obtained after subtraction of C_p obtained for superconducting EuCeSNCO (Fig. 12) as a background, assuming identical phonon contributions. The slope of this curve yields $\gamma = 420(5)$ mJ/mol K², a value which is only 10% higher than that deduced from the direct fit mentioned above. The upturn at $T < 2.5$ K is expected and is based on different relative values of the nuclear specific heat of Pr and Eu. For sample (II) the same procedure yields $\gamma = 157(2)$ mJ/mol K².

The average $\gamma = 265 \pm 15$ mJ/mol Pr K² for sample (I) compares well with values reported for PrBCO₇,¹⁹ but is somewhat higher than $\gamma = 200$ mJ/mol K² deduced by Phillips *et al.*²⁰ Although the average $\gamma = 108(10)$

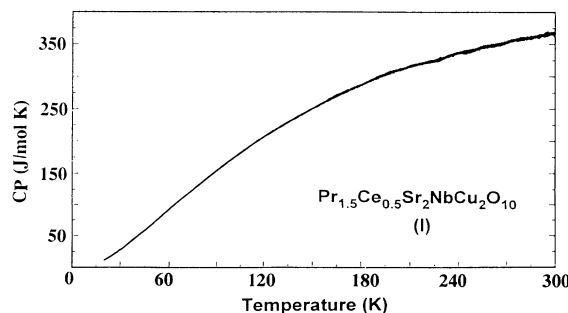


FIG. 11. Specific heat C_p for PrCeSNCO sample (I) at $H=0$ T as a function of temperature for $25 < T < 300$ K.

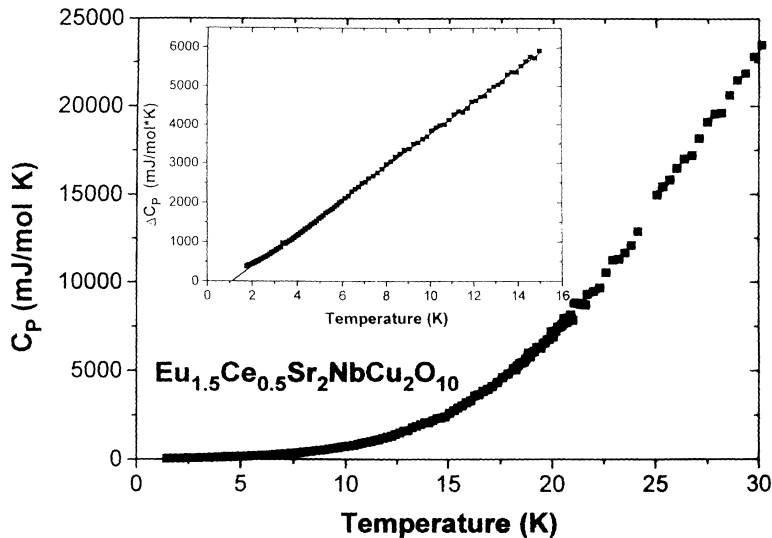


FIG. 12. Specific-heat curves at $H=0$ T for $\text{Eu}_{1.5}\text{Ce}_{0.5}\text{Sr}_2\text{NbCu}_2\text{O}_{10}$. The inset shows ΔC_p vs T for PrCeSNCO sample (I) (see text).

mJ/mol Pr K² obtained for sample (II) is lower than that of sample (I), it is still high enough to claim that in both PrCeSNCO materials the γ term is remarkably high.

The $C_p(T)$ data for EuCeSNCO in the range $1.5 < T < 16$ K can be described as the sum of three terms, the Eu Schottky anomaly, and the electronic and lattice terms discussed above. Thus, $C_p = A/T^2 + \gamma T + \beta T^3$. A fit to the curve shown in Fig. 12 yields $A = 20.7$ mJ K/mol, $\gamma = 18.9$ mJ/mol K², and $\beta = 0.416$ mJ/mol K⁴, corresponding to $\theta_D = 425(3)$ K. This relative high γ is in fair agreement with the value of $\gamma = 12.9$ mJ/mol K² obtained in $\text{EuBa}_2\text{Cu}_3\text{O}_7$.²¹ The failure to observe an anomaly in C_p related to the superconducting transition is usual for these materials and is discussed in detail in Ref. 19.

DISCUSSION

Our susceptibility measurements of PrCeSNCO sample (I), which are of central interest in the present paper, can be compared to the data reported in Ref. 11. Such a comparison is possible despite the fact that the measurements were performed on samples prepared in different laboratories and therefore have probably a slight difference in their oxygen content. We both observe two anomalies in the $\chi(T)$ curves measured at low applied fields, which are specific to PrCeSNCO, because no such transitions were observed in the superconducting RCeSNCO compounds.^{11–13} (The possibility that an impurity phase is the reason for those peaks was ruled out by Goodwin, Radousky, and Shelton¹¹ who concluded that even if a small amount of impurity with a large susceptibility and strong transition is present, its effect would be minimal on the already large χ of the bulk material.) For the peak at 54 K (Figs. 3–6) the results are consistent, and our MS data definitely indicate (Fig. 9) that this peak (although shifted to high temperatures) is due to AFM ordering of the Cu sublattice. Goodwin, Radousky, and Shelton¹¹ do not explain the peak at 53 K, but attribute the low-temperature peak observed at 17 K to the magnetic order of the Pr sublattice. The raw data

presented in Figs. 3–6 clearly show that in our material the low-temperature peak is obtained at 11 K (regardless of Fe concentration) and only in the “net” magnetic features of sample (I) does the broad anomaly exhibit a peak at 18 K (inset of Fig. 5). On the other hand, in the oxygen-rich material (HOP) both transitions are affected; the low one is shifted to 15 K and $T_N(\text{Cu})$ is lowered to 50 K (Fig. 3). This clearly indicates that both anomalies in the $\chi(T)$ curves are related to each other and appear always together. *Neither of them was observed separately.*

A. The effect of oxygen

The oxygen concentration has a drastic effect on the appearance of both anomalies. Sample (II) which contains less oxygen (Fig. 2) is paramagnetic down to 3 K and no magnetic transitions were detected in the $\chi(T)$ curve (Fig. 5). A similar behavior was observed in other RCeSNCO materials in which the occurrence of superconductivity strongly depends on the heat treatment and oxygen content.¹² The determination of the absolute oxygen concentration in these materials is difficult, and the critical oxygen content needed for the appearance of the magnetic transitions in PrCeSNCO (or superconductivity in RCeSNCO) has not yet been determined. Above this limit the effect of extra oxygen is not dramatic as can be observed in the HOP material (Fig. 3).

B. The difference between samples (I) and (II)

We can tentatively argue that the difference between the magnetic properties of samples (I) and (II) arises from the different valence state of Pr in the materials. One argument in favor of a tetravalent ground state for Pr in sample (I) is the effective moment ($P_{\text{eff}} = 2.53\mu_B$) deduced from measurements performed at 10 kOe in the temperature range $60 < T < 100$ K where $\chi(T)$ shows nearly perfect Curie-Weiss behavior [Fig. 6 (inset)]. This implies that the internal exchange field is much smaller than the applied field. On the other hand, P_{eff} obtained for sample (II) is higher and resembles the effective moment ob-

served in other Pr-based cuprates such as PrNBCO and PrBCO₇. For the latter compound all the most reliable spectroscopic studies reveal that Pr is trivalent.³ In that respect, sample (II) behaves similarly to the magnetically nonordered Pr₂CuO₄ in which Pr is trivalent. However the similar lattice parameters observed for both samples, together with the reduction observed in the lattice parameter of EuCeSNCO, suggest that Pr³⁺ is the more appropriate state to assume for both PrCeSNCO samples. Moreover, it was recently proved²² that this type of analysis is oversimplified for these complicated materials, and the P_{eff} 's obtained for Pr are fortuitous and cannot serve as a strong argument for the valency of Pr.

C. The effect of Fe

Fe has a huge effect on the position of $T_N(\text{Cu})$ (Fig. 4). The peak at 54 K is shifted to 74 or to 94 K, whereas the peak at 11 K is not affected by the presence of Fe (Fig. 4). Although, both doped materials denoted as samples Fe(I) and Fe(II) were prepared under identical conditions with the same nominal (0.5 at. %) ⁵⁷Fe concentration, one cannot exclude a tiny difference in their Fe content. $T_N(\text{Cu})$ may be affected either directly by the presence of Fe or indirectly by the change in oxygen concentration (less than 0.25%) attracted by Fe³⁺ to maintain neutrality. We may say with high confidence that the significant increase of $T_N(\text{Cu})$ is caused directly by the presence of Fe, to which it is very sensitive. In that respect, this system behaves completely differently from other magnetic high- T_c -based compounds, where doping with Fe does not affect $T_N(\text{Cu})$ and serves only as a probe for the magnetic order.^{2,14} Due to the low solubility of Fe in PrCeSNCO, our ability to study the effect of Fe concentration on $T_N(\text{Cu})$ is limited. Research on other substitutions is now in course of work. The alternative hypothesis (not preferable) raises two problems: (1) One has to distinguish between two sorts of oxygen atoms, those which reside in crystallographic positions and affect $T_N(\text{Cu})$ vigorously and others which were inserted into the structure during the high-pressure process (HOP) and occupy interstitial sites (their positions are not known) and practically do not affect the magnetic transition. (2) The extremely low probability that the two samples, our PrCeSNCO sample (I) and that reported in Ref. 11, although prepared under similar conditions, have exactly the same oxygen concentration.

D. The low $T_N(\text{Cu})$

In RBCO₆ the Cu ions in the CuO₂ planes are in a pyramidal configuration and order magnetically at $T_N \sim 420$ K, in a simple AFM structure with nearest-neighbor Cu(2) spins antiparallel in all three dimensions. In PrBNCO, a structure which is derived from RBCO, the Cu moments are AFM ordered⁸ below $T_N = 360$ K with a similar alignment to that of RBCO.⁹ On the other hand, in PrCeSNCO, we obtain $T_N(\text{Cu}) = 54$ K, and Fig. 1 shows that the CuO₂ layers are separated on one side by NbO₆ octahedra and on the other side by fluorite-

structured $R_{1.5}\text{Ce}_{0.5}\text{O}_2$ layers. The Cu-Cu short distance is about 6.1 Å, much longer than the 3.36 Å found in RBCO₆ and PrBNCO. It is thus possible to affect $T_N(\text{Cu})$ by inserting different separator layers between the CuO₂ planes which play an important role in the magnetic properties of the system.

E. The absence of a peak in C_p at $T_N(\text{Cu})$

The intriguing question arises as to why this AFM ordering of Cu in PrCeSNCO sample (I) does not cause any anomaly in the C_p curve (Fig. 11), despite the fact that a sizable magnetic entropy $S = R \ln 2 = 5.8$ J/mol K is normally expected for the ordering of Cu²⁺ spin with $s = \frac{1}{2}$. The unusual absence of a peak in C_p at T_N was also reported in Gd_{1.85}Ce_{0.15}CuO₄ (Ref. 23) and in La₂MCu₂O₆ (Ref. 17) systems, in which magnetic measurements and MS studies definitely show a long-range magnetic ordering of the Cu sublattices. This phenomenon, which differs markedly from other AFM ordered systems, can be understood on simple arguments. Let us recall that in the insulating Cu-O-based materials the AFM ordering of Cu moments can be modeled well by large AFM superexchange coupling ($J/k_B \sim 1000\text{--}1500$ K) between the Cu²⁺ spins ($s = \frac{1}{2}$) in the CuO₂ planes.²⁴ This strong intraplanar exchange yields large two-dimensional (2D) AFM correlations with dynamic short-range AFM ordering at temperatures much higher than T_N . In the 2D quantum Heisenberg model, a true long-range order cannot exist at finite temperatures. The *experimentally* observed AFM ordering at T_N is a three-dimensional (3D) one, driven by a relatively weak interplane coupling parameter $J_{\perp} \sim 10^{-5}\text{--}10^{-6}$ J. Due to this high anisotropy all magnetic entropy is effectively removed at $T > T_N$ through 2D quantum correlations, and the small fraction of entropy left at T_N is not sufficient to produce an anomaly in the specific-heat curves. The current magnetic results provide further support of such an interpretation. Figures 5–7 show that the susceptibility curves measured at different fields as well as the curves for sample (I) and sample (II) all merge at $T > 90$ K, well above $T_N = 54$ K. The initial curvature in the $M(H)$ curve measured at 60 K indicates also the existence of an internal field above T_N . All of these observations indicate that in layer-based materials with large anisotropy, the unusual C_p behavior is a consequence of strong 2D spin fluctuations.

F. The peak at $T < 15$ K in the susceptibility curve

In the absence of microscopic information, an interpretation of this peak is not straightforward. However we suggest two scenarios that could lead to the observed behavior. A central assumption is that Pr in PrCeSNCO sample (I) orders antiferromagnetically near 11 K, analogous to the Pr ordering at 17 and ~ 12 K in PrBCO₇ and PrBNCO.¹¹ In fact, in PrCeSNCO the Ce and Pr are distributed at random over the $4e$ crystallographic position, and its T_N should be compared rather with Pr_{0.75}R_{0.25}Ba₂Cu₃O₇ ($R = \text{Eu, Y}$) where $T_N \sim 12$ K.²⁵ Supporting evidence for this determination is: (1) the constant position at 11 K in the Fe-doped samples (Fig.

4), whereas the peak at elevated temperatures is very sensitive to Fe concentration and is affected by its presence. (2) In HOP material the peak shifts to 15 K in accordance with the trend found in PrBCO described in the Introduction. However, the absence of an anomaly in the C_p curve (Fig. 10) on one hand and the paramagnetic behavior of the oxygen-poor sample (Fig. 5) on the other cast some doubt on this interpretation. One approach to reconcile these difficulties is to propose a magnetic structure observed recently⁹ in PrNBCO⁹ where the Pr ordering is 2D in nature, and not 3D. The additional structure causes high anisotropy which leads to a weak interplanar coupling parameter and to a short-range order along the c axis. In such a case the magnetic transition is not detectable in the C_p curve, as discussed above.

A more preferable second interpretation can be made that invokes an analogy to Pr₂CuO₄, where the Pr sublattice is not magnetically ordered down to 2 K but the Cu sublattice orders AFM near 250 K. Therefore, for small applied fields at low temperatures, the most prominent features in the data of Figs. 3–7 are not associated with AFM order of Pr but are related to the presence of other effects, e.g., Pr-Cu and Cu-Cu interactions. The peak at low temperature is always accompanied by the transition at high temperatures and can be interpreted in the light of understanding the magnetic interactions responsible for the high-temperature peak. Since the detailed 2D AFM structure of the Cu sublattice is not yet determined, we may assume that the Cu moments are not in a perfect AFM structure at $T < T_N(\text{Cu})$. There might be a canting of Cu moments from strictly AFM alignment, of unknown origin. Due to the large susceptibility of Pr, the canting moment is not observable in the $\chi(T)$ curves. At low temperature the Cu-Cu and/or Pr-Cu interactions

begin to dominate, leading to reorientation of the Cu moments and the anomaly in the susceptibility is observed. This scenario is supported by: (1) the broad peak in the inset of Fig. 5; (2) the lack of transition in the FC branch (Fig. 7), where the aligned component of the Cu moments along the field direction inhibits the reorientation; (3) the prevention of the reorientation by high applied fields; (4) the fact that this reorientation, which is independent of $T_N(\text{Cu})$, leads to a negligibly small latent heat which cannot be observed in the C_p curve.

As a final point of interest, we may discuss the high linear terms for the electronic specific heat observed in $C_p(T)$ for PrCeSNCO materials. The values $\gamma = 265$ and $108 \text{ mJ/mol Pr K}^2$ were obtained for samples (I) and (II) respectively. The γ value observed for sample (I) is higher than that reported by Phillips *et al.*²⁰ for PrBCO and compares well with values reported in Ref. 19. If we adopt the first scenario for the magnetic peak at $T = 11 \text{ K}$ in sample (I), it is reasonable to assume that the high $T_N(\text{Pr})$ and the anomalously high γ term are connected. However, for the second scenario the high γ values need some more consideration.

ACKNOWLEDGMENTS

Discussions with Professor B. Raveau are acknowledged. We wish to express our sincere thanks to C. Martin for preparing samples under high oxygen pressure. One of us (I.F.) is indebted to Kernforschungszentrum Karlsruhe (INFP) for hospitality in the early stage of this research. The research was supported by the Israeli Ministry of Science and Technology, by the Klachky Foundation for Superconductivity, and by the US-Israel Binational Science Foundation (BSF) 1993.

¹W.-H. Li *et al.*, Phys. Rev. B **40**, 5300 (1989).

²I. Felner *et al.*, Phys. Rev. B **40**, 6739 (1989).

³H. B. Radousky, J. Mater. Res. **7**, 1917 (1992).

⁴G. Wortmann and I. Felner, Solid State Commun. **75**, 981 (1990).

⁵A. Ichinose *et al.*, J. Ceram. Soc. Jpn (Int. Ed.) **97**, 1053 (1989).

⁶M. Bennahmias *et al.*, Phys. Rev. B **46**, 11 986 (1992).

⁷H. Jhans, S. K. Malik, and R. Vijayaraghavan, Solid State Commun. **85**, 105 (1993).

⁸I. Felner *et al.*, Physica C **214**, 169 (1993).

⁹N. Rosov *et al.*, Phys. Rev. B **47**, 15 256 (1993).

¹⁰L. Rukang, Z. Yingjie, A. Yitai, and C. Zuyao, Physica C **176**, 19 (1991).

¹¹T. J. Goodwin, H. B. Radousky, and R. N. Shelton, Physica C **204**, 212 (1993).

¹²R. J. Cava *et al.*, Physica C **191**, 237 (1992).

¹³W. Shiwei *et al.*, Physica C **210**, 463 (1993).

¹⁴I. Felner *et al.*, Phys. Rev. B **46**, 9132 (1992).

¹⁵M. F. Lopez-Morales *et al.*, Phys. Rev. B **41**, 6655 (1990).

¹⁶I. Felner *et al.*, Phys. Rev. Lett. **65**, 1945 (1990).

¹⁷I. Felner *et al.*, Phys. Rev. B **47**, 12 190 (1993).

¹⁸A. Junod, in *Physical Properties of High T_c Superconductors II*, edited by D. M. Ginsberg (World Scientific, Singapore, 1990), p. 13.

¹⁹S. Ghamaty *et al.*, Phys. Rev. B **43**, 5430 (1991).

²⁰N. E. Phillips, *et al.*, Phys. Rev. B **43**, 11 488 (1991).

²¹J. M. Ferreira *et al.*, Phys. Rev. B **37**, 1580 (1988).

²²G. Hilscher *et al.*, Phys. Rev. B **49**, 535 (1994).

²³G. H. Hwang, J. H. Shieh, J. C. Ho, and H. C. Ku, Physica C **201**, 171 (1992).

²⁴A. Aharony *et al.*, Phys. Rev. Lett. **60**, 1330 (1988); H. Alloul *et al.*, Physica C **171**, 419 (1990).

²⁵G. Nieva *et al.*, Phys. Rev. B **44**, 6999 (1991).